

# Submersible Installed Permanent Magnet Synchronous Motor for a Photovoltaic Pump System

S. Van Haute, St. Henneberger, K. Hameyer and R. Belmans  
Katholieke Universiteit Leuven E.E. Dept., Div. ESAT/ELEN  
Kardinaal Mercierlaan 94, B-3001 Leuven - Heverlee, Belgium

**Abstract:** Nowadays, an increasing request for more powerful photovoltaic irrigation systems can be stated. A 3.8 kW permanent magnet synchronous motor (PMSM) is designed to meet the requirement of such type of drive system. The higher efficiency of PMSMs when compared to induction motors is shown and reduces the number of required PV modules. A standard induction motor having a squirrel cage rotor and a permanent magnet (PM) motor are studied. A rotor cage is constructed for the PM rotor for open loop operation. The motor is controlled by a modified standard PWM inverter, equipped with selectable constant voltage or maximum power point (MPP) tracking algorithms. Special attention is paid to meet all system requirements.

**Keywords:** photovoltaic pump system, irrigation system, maximum power point tracking, permanent magnet motor, PWM inverter.

## I. INTRODUCTION

Photovoltaic (PV) pump systems are used to satisfy drinking water and irrigation needs (Fig.1). Several systems have been developed recently [1-3]. Surface applications for irrigation systems are driven by permanent magnet dc machines while for submerged motor-pump units induction machines are used. However, small induction motors have, when compared with permanent magnet motors, a lower efficiency, whereas dc machines are not applicable for submerged installations.

Most of the currently operated photovoltaic irrigation systems offer a mechanical output power in the range of 0.85 kW up to 2.2 kW [1]. For higher system power ratings the cost of the photovoltaic array increases substantially. However, these larger systems offer major opportunities for increasing the overall system efficiency. Due to the fact that the cost of a photovoltaic array accounts for a substantial fraction (25-50%) of the overall installed pump system cost[1], a higher system efficiency can induce an important cost reduction. Although the overall system efficiency is determined by the optimum matching of all system components (Fig. 2), increased

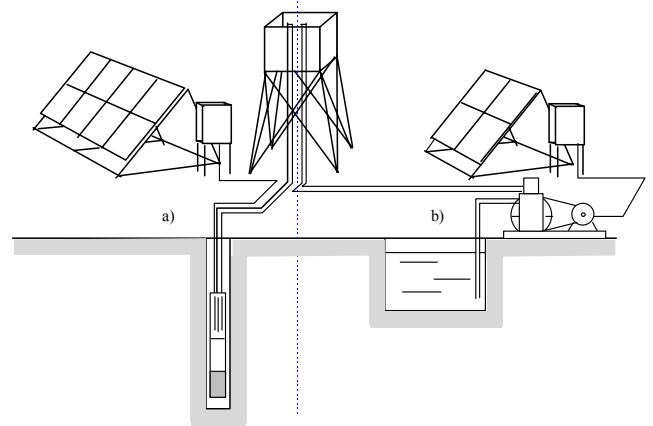


Fig. 1. Photovoltaic pump systems  
a) submerged motor pump unit and b) surface application.

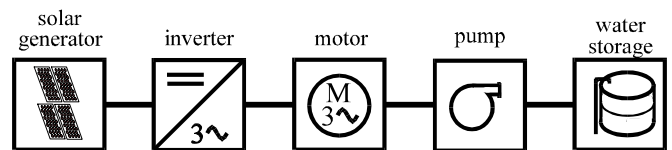


Fig. 2. Main components of a photovoltaic pump system.

efficiency of one component of the system contributes to the overall result.

The installed output power of the solar cells may be decreased by using permanent magnet excited motors and is profitable for relatively high system power ratings. Therefore, a 3.8 kW PMSM for submersible installations is designed and developed for open loop operation by employing a rotor cage in order to avoid a position sensor and closed loop operation. The design process combines analytical calculations with the finite element method (FEM).

In order to get experience on this kind of motor a standard 3.2 kW induction motor is modified by applying a new stator winding and a new rotor containing surface mounted permanent magnets and a rotor cage. The motor is controlled by a modified standard inverter with selectable operation modes. Experimental results from the drive are compared with induction motor performance for a typical PV configuration.

## II. THE PHOTOVOLTAIC ARRAY

The installed power and configuration of the photovoltaic array has to be designed as such that it is matched with the inverter, motor and pump to obtain a maximum water output under the given meteorological conditions. The series and parallel connection of the photovoltaic modules is determined by the nominal input power and allowed voltage range at the inverter.

Fig. 3 shows the daily evolution of the global irradiance on a tilted plane of  $10^\circ$  for the site of Bamako in Mali ( $12^\circ$  N,  $8.4^\circ$  E) which is representative for the envisaged application circumstances of the system. Fig. 4 is the result of simulations of a normalised photovoltaic system of 1 kWp. It represents a histogram that indicates the distribution of the DC energy at the array output as a function of the DC power. Based on this graph, water output calculations are performed and optimized for different configurations. For the motor with a rated power of 3.8 kW the optimum photovoltaic array has a peak power of 5.5 kWp to 6 kWp.

It is chosen to implement a nominal PV array voltage of 270 V DC which corresponds to a rated fundamental motor voltage of 190 V. The relatively high DC voltage is chosen in

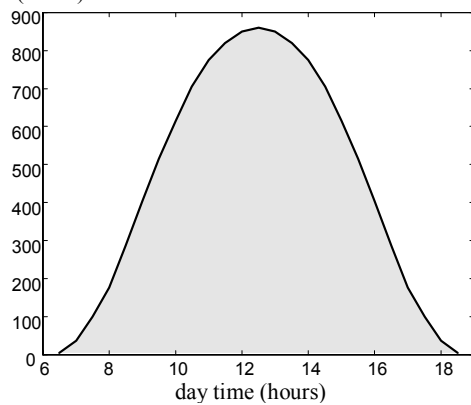


Fig. 3. The distribution of the in-plane solar irradiation over a day at the site of Bamako (Mali).

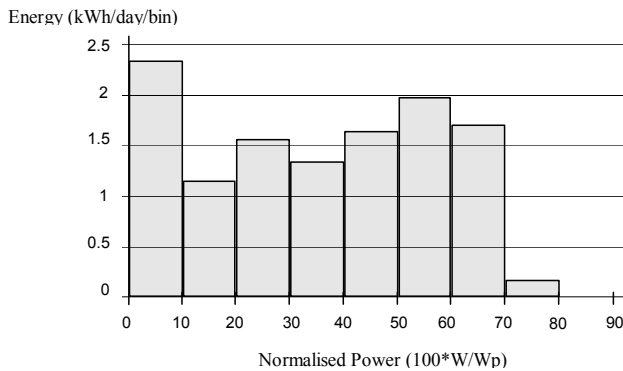


Fig. 4. The distribution of the energy of the PV array is given over the normalised power at the array for the site of Bamako (Mali).

order to limit the current, reducing not only the motor size and the cost of the semi-conductor components for the inverter but also the inverter losses and the conduction losses in the PV array. Special safety precautions have to be taken to apply these voltages without inducing higher personal risk.

The photovoltaic array consists of 6 parallel strings of 17 standard modules of 55 Wp, connected in series, resulting in a peak power of 5.6 kWp.

## III. INVERTER AND CONTROL

No commercially available inverter for solar generators fulfils the combined requirements of the envisaged system. This is because of a limited input voltage range, inverter standardisation for induction motors and a limited output frequency [3]. However, the development and assembly of a completely new inverter would increase substantially the cost of the overall photovoltaic pump system. Therefore, a standard VSI-PWM IGBT inverter is modified and adapted, adding maximum power point (MPP) tracking and specific protection measures, ensuring reliable operation under severe conditions. It is mounted on a water cooled backplane body and can be placed in an IP55 protection enclosure. Because of use in rural environments, only a few relevant functions can be altered from the outside after installing the system.

The V/f control is adapted to the PMSM. As the input DC voltage is not constant, the standard PWM strategy is modified to supply the motor with the maximum voltage that can be generated from a given DC input voltage.

Because the pump system is aimed to have maximum performance, it is important that a suitable control algorithm is implemented. Therefore the inverter used for the laboratory tests can operate in three modes:

- constant voltage operation;
- constant voltage operation with feedback of PV array temperature;
- maximum power point tracking.

Fig. 5 illustrates these modes of operation. It shows typical I-V curves for one module at different levels of irradiance and at constant cell temperature. The control algorithm can force the load to operate at a preselected DC inverter input voltage. This voltage can be chosen within a certain range to adapt to a given PV array configuration (indicated by the vertical lines).

As the I-V curves of the array shift also horizontally with cell temperature, the constant voltage tracking mode can be extended using cell temperature feedback (not shown in Fig.5).

The third mode is a continuous maximum power point tracking. This means that at each instant of time the maximum available power from the PV array is used by the load. The locus of maximum power points is indicated. It can be seen

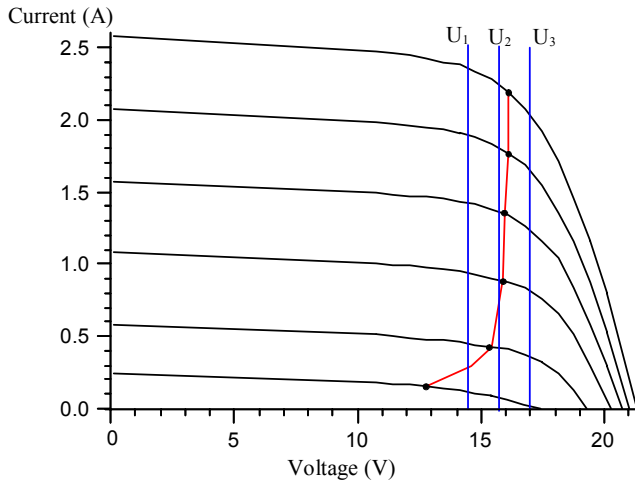


Fig. 5 PV module I-V curves with maximum power point locus and selected voltages for constant voltage operation

TABLE 1  
NORMALISED OUTPUT FOR THE SITE IN MALI

	kWh/kWp
MPPT	1661
CVT	1636
CVT with T-feedback	1641

that under ideal conditions and for an appropriate choice of the DC voltage, the constant voltage tracking can perform quite well. However, in practice, effects of shadowing and aging, besides the changing cell temperature, causes the PV characteristics to change. This means that the MPP tracking algorithm is superior when compared to the constant voltage tracking methods.. Table 1 gives a simulated output for the three power control methods.

#### IV. MOTOR DESIGN

To obtain a maximum water output over the course of the day, PV pump systems should reach a high conversion efficiency even at low irradiation levels (Fig. 3). This corresponds to the requirement to operate the motor with low losses in a large power range.

By studying the drive concept (Fig. 2) it is obvious that the motor is the only component where a relatively high improvement of the overall efficiency can be realised. Furthermore the adaptation of the motor to the pump as well as to the inverter is considered in order to obtain a high efficiency of the drive system.

#### A. Permanent magnets

The high energy permanent magnet material NdFeB offers a high energy density as well as a high remanence flux density. A high remanent flux density is needed, while a high coercivity is less important as overloads do not occur. Furthermore, motors with higher temperatures are no longer a drawback as the new generation of NdFeB magnets retains its magnetic properties up to high temperatures. Using surface mounted magnet blocks, fixed onto the rotor, instead of one magnet shell per pole, reduces the eddy current losses and the heating up of the magnets.

#### B. PM rotor with additional damper cage

Besides the permanent magnets, the rotor has to carry a damper cage in order to enable the motor to operate in open loop. Therefore, the angular magnet width is restricted to leave space for the rotor bars. To maximise the influence of the rotor bars, the air gap between the magnets, has to be larger than the opening of the rotor slots. Thus, the motor has a significant saliency and can be compared to a machine with surface-inset magnets [6] (Fig. 6). An advantage of the surface inset structure is that the torque giving force on the magnets is transferred to the rotor core by the iron between the magnets [7]. Furthermore the rotor surface can be smooth being rather important for the banding. A disadvantage of this surface-inset type is an increased magnetic leakage flux. Also a higher torque ripple is caused by the saliency.

The rotor bars are narrowing the flux path and thus saturation of the q-axis may occur. These saturation effects can not be calculated analytically and are computed using FEM. Fig. 7 shows the flux plot of the magnetostatic solution of the PMSM under rated conditions. The computed torque differs less than one percent from the analytical calculations, meaning that the machine is not highly saturated. The calculated motor ratings are collected in Table 2.

#### V. MAGNETOSTATIC CALCULATION OF THE EQUIVALENT CIRCUIT

The high efficiency at partial load is shown by calculating the operating points of the equivalent circuit of the machine. As in irrigation systems no strong dynamic requirements are present, a static solution is sufficient. The results are summarised in table 3.

TABLE 2  
MOTOR PARAMETERS AT STEADY STATE

Motor parameter	Data
Number of poles	$2p = 4$
Rated speed	2240 rpm
Rated voltage	190 V
Rated current	14.8 A
Mechanical power (at 2200 rpm)	3480 W
Mechanical torque	14.8 Nm
Efficiency	92.2 %

TABLE 3  
OPERATING POINTS OF THE EQUIVALENT CIRCUIT

U	n	I	$T_m$	$P_m$	$\eta$
0.5 $U_n$	1068	$I_n$	16.13	1.80	87.24
0.6 $U_n$	1300	$I_n$	16.11	2.19	89.06
0.7 $U_n$	1533	$I_n$	16.10	2.58	90.36
0.8 $U_n$	1765	$I_n$	16.09	2.97	91.31
0.9 $U_n$	1998	$I_n$	16.07	3.36	92.05
1.0 $U_n$	2230	$I_n$	16.06	3.75	92.62
1.1 $U_n$	2463	$I_n$	16.04	4.14	93.07

## VI. MODIFIED INDUCTION MOTOR

In order to compare an induction motor to a PMSM, a 3.2 kW standard induction motor is modified by applying a new stator winding and a new rotor containing permanent magnets and an incomplete rotor cage (Fig. 6). To obtain detailed information on the behaviour of a PMSM operating in open loop and supplied by a standard inverter for induction motors, was the main object of this part of the study. The higher efficiency of the permanent magnet motor can be shown if the newly constructed rotor is compared to the original standard rotor of the induction machine, both having the same stator.

The experimental tests state a smooth start up of the drive as required and predicted. Measurements show that due to the new stator winding the point of maximum efficiency of the induction motor has shifted towards lower load regions (Fig. 8). However, the efficiency of the motor with the permanent magnet rotor is distinctly higher in the interesting torque range, when compared to the squirrel cage rotor. This means that for the same output of pumped water, less PV modules are required.

## VI. PUMP LOAD MATCHING AND SYSTEM EFFICIENCY

According to the envisaged installed power range, a centrifugal pump is chosen. Considering the constraints set by the PMSM, the pump has the highest efficiency in the range of 1500 to 2200 rpm and a maximum mechanical power of 4 kW (Fig. 10). The optimum working conditions of this pump are found at a total manometric head between 12 and 18 m (Fig. 9). However, this can be adapted by adjusting the impeller.

For a typical manometric head of 15 m, the inverter-motor-pump combination has an overall efficiency of more than 50 % between 1,5 and 4 kW mechanical output power. with a maximum near 60 %. During a long period of the day, the system is working in this power range (Fig 3). At very low power levels, the system efficiency deteriorates mainly due to the inevitable strong decrease of the pump efficiency.

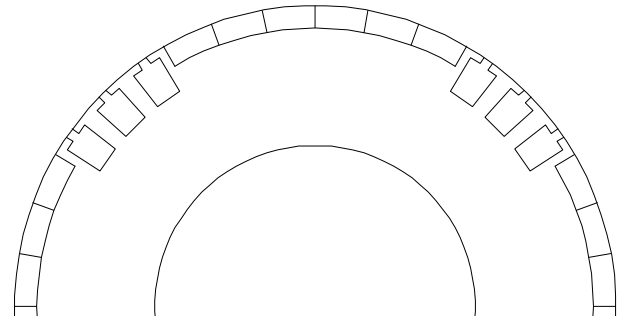


Fig. 6. Part of a cross sectional view of the 4-pole rotor.

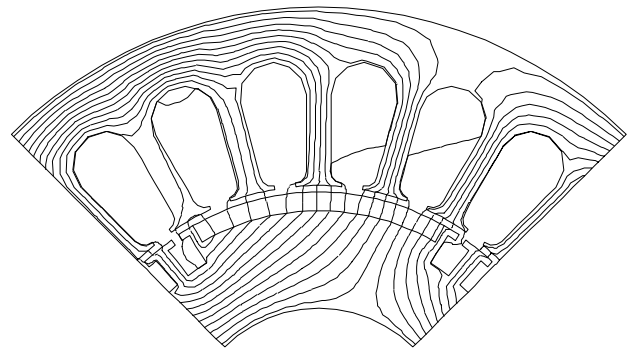


Fig. 7. Flux lines for the PMSM with rotor bars between the permanent magnet poles.

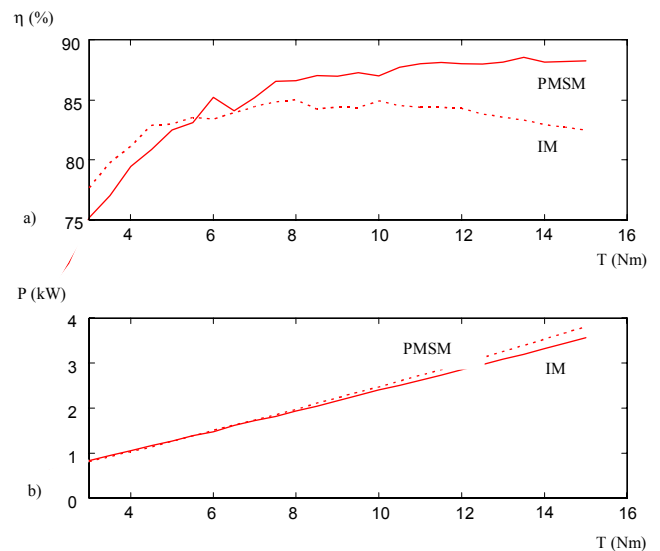


Fig. 8 Comparison of experimental results of the permanent magnet and the squirrel cage rotor  
a) efficiency and b) output power versus torque

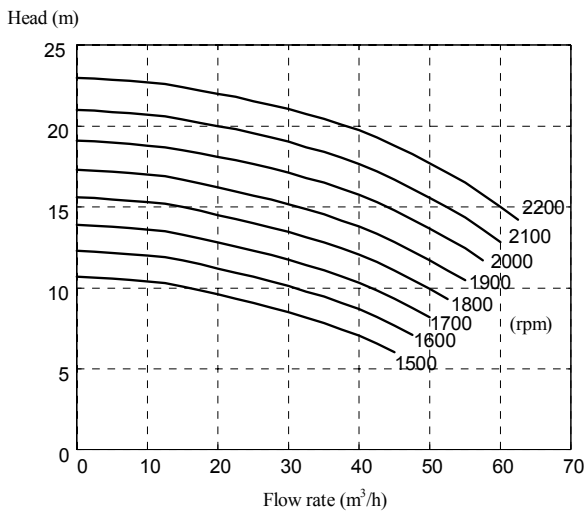


Fig. 9 Pump characteristics at different rotational speeds

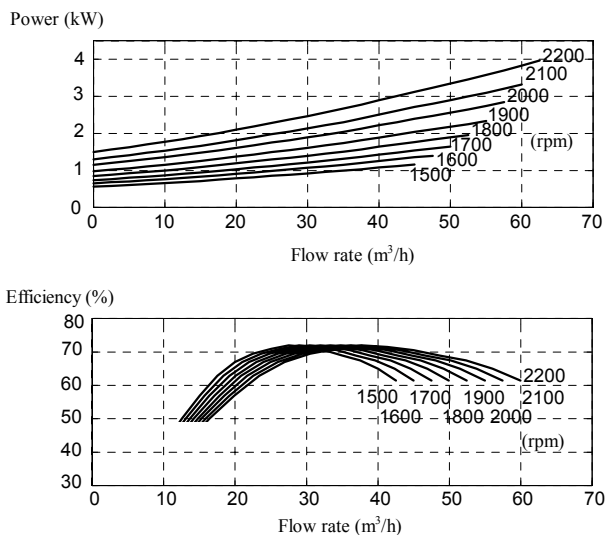


Fig. 10 Mechanical power and pump efficiency as a function of the flow rate

## VIII. CONCLUSIONS

In this paper the design of a PMSM for a photovoltaic irrigation system is presented. The aim to get a high efficiency water pump system has been reached by matching motor and pump and using maximum power point tracking. Rotor bars have been implemented to allow open loop operation and to balance disturbances. A standard PWM inverter is modified to be supplied from a PV array and to control the PMSM.

## IX. ACKNOWLEDGEMENTS

The authors are indebted to the Belgian Ministry of Scientific Research for granting the project IUAP No. P4/20 on Coupled Problems in Electromagnetic Systems. Furthermore, the research is supported by Flanders' Secretary of Economy.

## X. REFERENCES

- [1] Ph. Malbranche, J.M. Servant, A. Hänel, and P. Helm, "Recent developments in PV pumping applications and research in the European Community," *Proceedings of the 1994 European Photovoltaic Solar Energy Conference*, pp. 476-481
- [2] R. Barlow, B. McNelis and A. Derrick, "Status and experience of solar PV pumping in developing countries," *Proceedings of the 1991 European Photovoltaic Solar Energy Conference*, pp. 1143-1146
- [3] S. Makukatin, "Water from the African sun," *IEEE Spectrum*, October 1994, pp. 40-43
- [4] L. Chang., G.R. Dawson and T.R. Eastham, "Permanent magnet motor design: finite elements and analytical methods," *Proceedings of the 1990 International Conference on Electrical Machines*, pp. 1082-1088.
- [5] G.R. Slemon and L. Xian, "Modelling and design optimisation of permanent magnet motors," *Electric Machines and Power Systems*, vol. 20, no. 2, April 1992, pp. 71-92.
- [6] S.A. Nasar, I. Boldea and L.E. Unnewehr, *Permanent Magnet, Reluctance, and Self-Synchronous Motors*, London-Tokyo: CRC Press, 1993
- [7] E. Nipp, "Alternative to field weakening of surface mounted permanent magnet motors for variable speed drives," *Proceedings of the 1995 Industrial Applications Society*, pp. 191-198.
- [8] T. Sebastian., G.R. Slemon and, M.A. Rahman, "Design considerations for variable speed permanent magnet motors, *Proceedings of the 1986. International Conference on Electrical Machines*, pp. 1099-1102.

## X. BIOGRAPHIES



**Stefaan A.R. Van Haute** received the M.S. degree in electrical engineering in 1991 from the Katholieke Universiteit Leuven (K.U.Leuven), Belgium.

In October 1991 he started working in the Electrical Engineering Department (ESAT) of the same university as a teaching assistant. In 1993 he obtained an additional degree in managerial economics. Since October 1993 he is active as a research assistant in the electrical energy research group (ESAT-ELEN). His research interests are mainly in the field of electrical machines and variable speed drives, including control and energy optimization of industrial drive systems. Currently he is working on the control of non-conventional supplied drives. The research work includes DSP-based control of inverter-fed permanent magnet synchronous motors.



**Stefan Henneberger** was born in Mannheim, Germany, on March 9, 1966. He studied at the technical University in Aachen, Germany from 1987-1992, where he received his M.S. degree in electrical engineering.

Since 1993 he is working as research assistant at the Electric Energy Research Group of the Katholieke Universiteit Leuven, Belgium, working on his Ph.D. degree. His special field of interest is the design, development and simulation of permanent magnet drives.



**Kay Hameyer** (M' 1995) received the M.S. degree in electrical engineering in 1986 from University of Hannover, Germany. He received the Ph.D. degree from University of Technology Berlin, Germany, 1992.

From 1986 to 1988 he worked with the Robert Bosch GmbH in Stuttgart, Germany, as a design engineer for permanent magnet servo motors. In 1988 he became a member of the staff at the University of Technology Berlin, Germany. From November to December 1992 he was a visiting professor at the COPPE Universidade Federal do Rio de Janeiro, Brazil, teaching electrical machine design. In the frame of a collaboration with the TU Berlin, he was in

June 1993 a visiting professor at the Université de Batna, Algeria. Beginning in 1993 he was a scientific consultant working on several industrial projects. From 1993 to March 1994, he held a HCM-CEAM fellowship financed by the European Community at the Katholieke Universiteit Leuven, Belgium. Currently he is professor for numerical field computations with the K.U.Leuven and a senior researcher with the F.W.O.-V. in Belgium, teaching CAE in electrical engineering and electrical machines. His research interests are numerical field computation, the design of electrical machines, in particular permanent magnet excited machines and numerical optimization strategies.

Dr. Hameyer is member of the International Compumag Society.



**Ronnie J.M. Belmans** (S'77-M'84-SM'89) received the M.S. degree in electrical engineering in 1979 and the Ph.D. in 1984, both from the Katholieke Universiteit Leuven, Belgium, the special Doctorate in 1989 and the Habilitation in 1993, both from the RWTH Aachen, Germany.

Currently, he is a full professor with the K.U. Leuven, teaching electrical machines and CAD in magnetics. His research interests include electrical machine design (permanent magnet and induction machines), computer aided engineering and vibrations and audible noises in electrical machines. He was the director of the NATO Advanced Research Workshop on

Vibrations and Audible Noise in Alternating Current Machines (August 1986). He was with the Laboratory for Electrical Machines of the RWTH Aachen, Germany, as a Von Humboldt Fellow (October 1988-September 1989). From October 1989 to September 1990, he was visiting professor at the McMaster University, Hamilton, ON., Canada. He obtained the chair of the Anglo-Belgian Society at the London University for the year 1995-1996.

Dr. Belmans is a member of the IEE (U.K.), the International Compumag Society and the Koninklijke Vlaamse Ingenieursvereniging (KVIV).

### C. Simulation

The asymmetrical rotor cage has to ensure the start up of the V/f controlled motor and to balance disturbances. The start up is simulated by combining a PMSM as well as an induction machine. The dimensions of the rotor bars are calculated by computing the resistance and the current they have to carry requiring a cross section of about 20 mm<sup>2</sup>.

In the start up procedure a slip is given, corresponding to the required start up current. The rotor frequency  $f_2$  has to fulfil the equation  $f_2 = f_1 + p \cdot n$ . If the machine has reached its synchronism  $f_2$  is set to zero (Fig. 7).

Figure 8a shows the smooth start of the motor up to the demanded speed. The asynchronous torque becomes zero if the machine has reached the synchronism. Then the induced voltage tunes in on its stationary value (Fig. 8b).

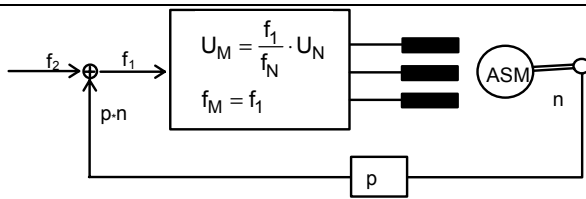


Fig. 7. Control scheme of the simulation of the start up procedure.

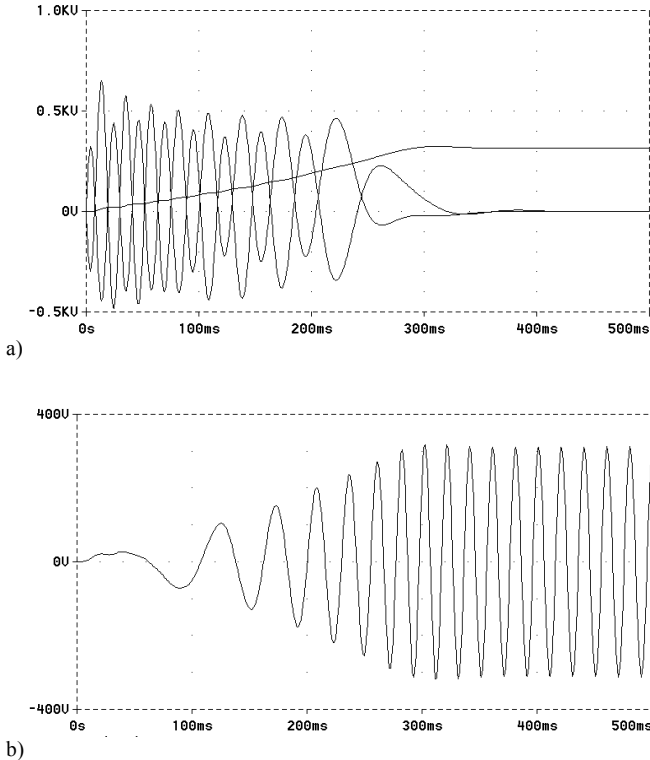


Fig. 8. Start up of the PMSM a) induced voltage and b) asynchronous torque and the speed versus time.

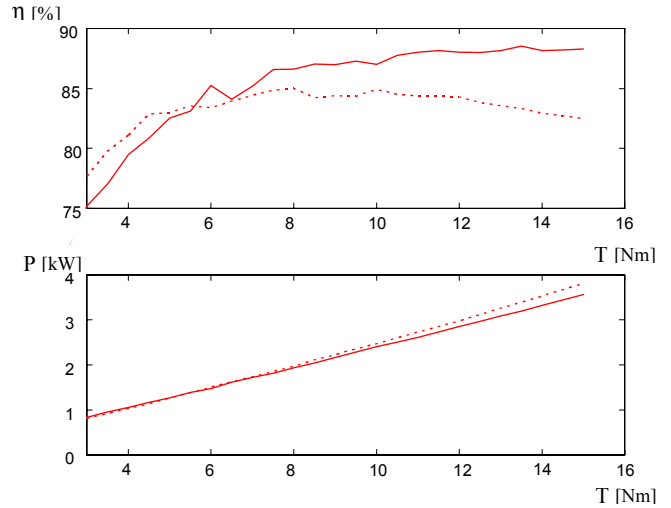


Fig. 9 Comparison of experimental results of the permanent magnet and the squirrel cage rotor : a) efficiency and b) output power versus torque

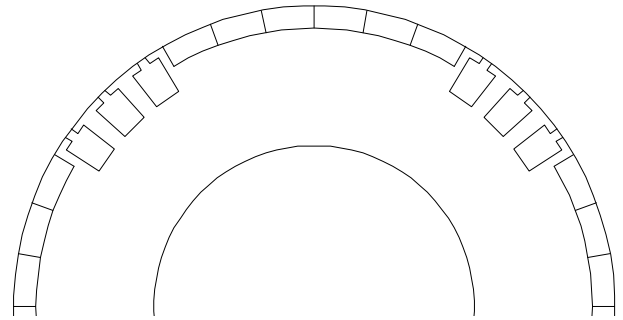


Fig. 5. Part of a cross sectional view of the 4-pole rotor.

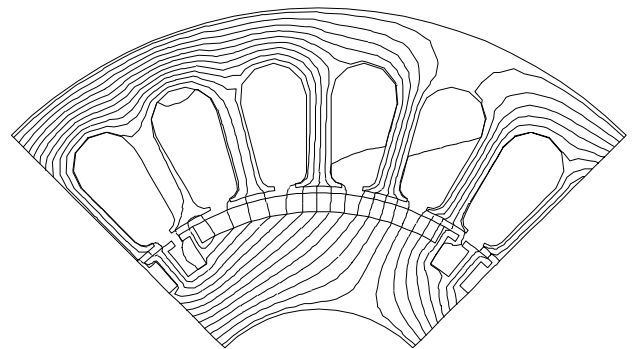


Fig. 6. Flux lines for the PMSM with rotor bars between the permanent magnet poles.

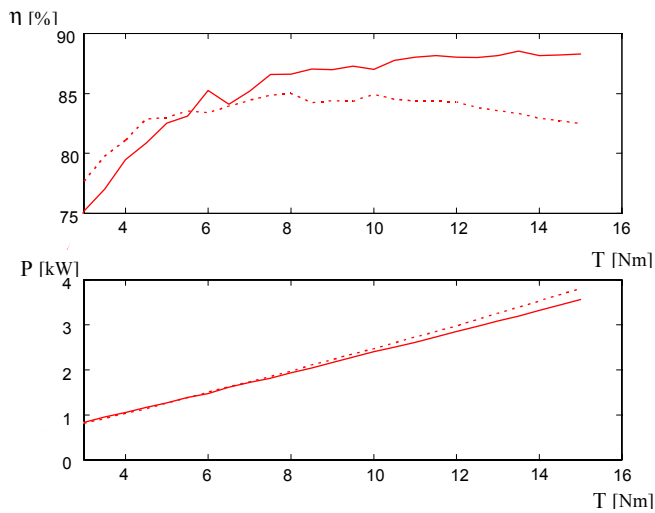


Fig. 7 Comparison of experimental results of the permanent magnet and the squirrel cage rotor : a) efficiency and b) output power versus torque



**Stefaan A.R. Van Haute** received the M.S. degree in electrical engineering in 1991 from the Katholieke Universiteit Leuven (K.U.Leuven).

He started working in the Electrical Engineering Department (ESAT) of the same university as an assistant. In 1993 he obtained an additional degree in managerial economics. Since October 1993 he is active as a research assistant in the electrical energy research group (ESAT-ELEN). His research interests are mainly in the field of electrical machines and variable speed drives, including control and energy optimization of industrial drive systems. Currently he is working on the control of non-conventional supplied drives. The research includes also DSP-

based control of inverter-fed permanent magnet synchronous motors.

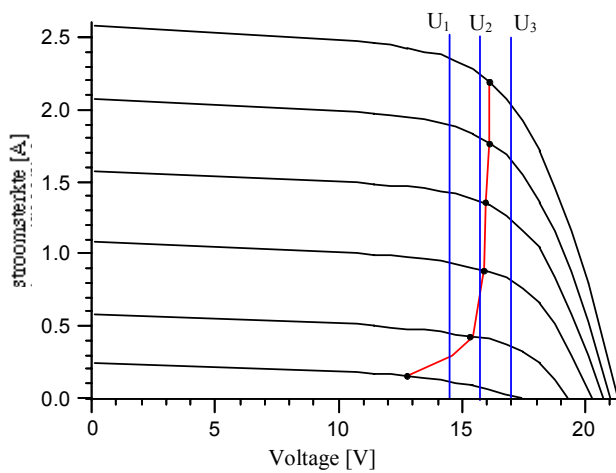


Fig. 10 I-V curves with maximum power point locus and selected voltages for constant voltage operation

TABLE III  
NORMALISED OUTPUT FOR THE SITE IN MALI

	kWh/kWp
MPPT	1661
CVT	1636
CVT with T-feedback	1641

TABLE 2  
MOTOR PARAMETERS AT STEADY STATE

Motor parameter	Data
Number of poles	$2p = 4$
Rated speed	2240 rpm
Rated voltage	190 V
Rated current	14.8 A
Mechanical power (at 2200 rpm)	3480 W
Mechanical torque	14.8 Nm